

This is the accepted manuscript made available via CHORUS. The article has been published as:

Topological insulators on a Mobius strip

Lang-Tao Huang and Dung-Hai Lee

Phys. Rev. B **84**, 193106 — Published 29 November 2011

DOI: [10.1103/PhysRevB.84.193106](https://doi.org/10.1103/PhysRevB.84.193106)

Topological insulators on a Mobius Strip

Langtao Huang¹ and Dung-Hai Lee^{2,3}

¹*Department of Physics, Tsinghua University, Beijing 100084, China;*

²*Department of Physics, University of California at Berkeley, Berkeley, CA 94720, USA;*

³*Materials Sciences Division, Lawrence Berkeley National Laboratory, Berkeley, CA 94720, USA.*

(Dated: November 10, 2011)

We study the two dimensional Chern insulator and spin Hall insulator on a non-orientable Riemann surface, the Mobius strip, where the usual bandstructure topological invariant is not defined. We show that while the flow pattern of edge currents can detect the twist of the Mobius strip in the case of Chern insulator, it can not do so in spin Hall insulator.

Band insulator with interesting bandstructure topology, the so called “topological insulator”, has attracted considerable attention lately¹. Mathematically these free-electron insulators are characterized by topological invariants in their bandstructure. Examples include the Chern number^{2,3} and Z_2 index⁴⁻⁷ for the Chern and Z_2 insulator, respectively. Physically a hallmark of these insulators is their protected boundary states. In two dimensions these are the chiral edge states of the integer quantum Hall effect^{8,9}, and the helical edge states of the spin Hall insulator^{10,11}. In three dimensions the boundary states have a massless Dirac fermion dispersion relation^{12,13}.

In this paper we ask a simple question: in two dimensions can we put topological insulators on a non-orientable Riemann surface? and if so, what are their signatures? The first question was posed to us by Prof. X. Sun of the Fudan University. Clearly the usual bandstructure topological invariants can not be defined in this situation; therefore naturally one would examine the edge state structure. In the following we study two dimensional Chern and Z_2 insulator on the Mobius strip. Since the Mobius strip has only one edge, it is far from clear how does the flow pattern of the current look like.

First we start with the Chern insulator. As pointed out by Haldane¹⁴, the necessary ingredient of Chern insulator is time-reversal symmetry breaking rather than net magnetic flux. Specifically we consider the following two-band model on square lattice

$$\mathcal{H}(\mathbf{k}) = \mathbf{d}(\mathbf{k}) \cdot \vec{\tau}. \quad (1)$$

Here $\vec{\tau}$ are Pauli matrices which acts on the (two) orbital degrees of freedom, and

$$\mathbf{d}(\mathbf{k}) = (\sin k_x, \sin k_y, 1 - \cos k_x - \cos k_y). \quad (2)$$

It is straightforward to check that the Chern number (or the TKKN index) associated with the valence band of this model is 1. In order to implement this model on the Mobius strip we first need to Fourier transform the above model to real space:

$$H = -\frac{1}{2} \sum_{i,j} \left[i(\psi_{i+1,j}^\dagger \tau^x \psi_{i,j} + \psi_{i,j+1}^\dagger \tau^y \psi_{i,j}) + \psi_{i+1,j}^\dagger \tau^z \psi_{i,j} + \psi_{i,j+1}^\dagger \tau^z \psi_{i,j} + h.c. \right] + \sum_{i,j} \psi_{i,j}^\dagger \tau^z \psi_{i,j}. \quad (3)$$

In the above (i, j) are the integer coordinates of the sites of a square lattice, and ψ is a two-component fermion field associated with the two orbitals in question. Because we shall study Eq. (3) on the Mobius strip it is essential to define how the orbitals couple to the local

orientation. A convenient definition is to let the pseudospin corresponding to the orbital degrees of freedom couple to space curvature in the same way the real spin in Dirac theory does¹⁵. This amounts to replacing the τ matrices in Eq. (3) by position-dependent Pauli matrices, i.e.,

$$H = -\frac{1}{2} \sum_{i,j} \left[i(\psi_{i+1,j}^\dagger \tau_{i,j}^x \psi_{i,j} + \psi_{i,j+1}^\dagger \tau_{i,j}^y \psi_{i,j}) + \psi_{i+1,j}^\dagger \tau_{i,j}^z \psi_{i,j} + \psi_{i,j+1}^\dagger \tau_{i,j}^z \psi_{i,j} + h.c. \right] + \sum_{i,j} \psi_{i,j}^\dagger \tau_{i,j}^z \psi_{i,j}. \quad (4)$$

where

$$\vec{\tau}_{i,j}^\mu = \hat{n}_{i,j}^\mu \cdot \vec{\tau}. \quad (5)$$

Here $\mu = 1, 2, 3$ and $\hat{n}_{i,j}^\mu$ are unit vectors defining a local frame when the relevant surface is embedded in the

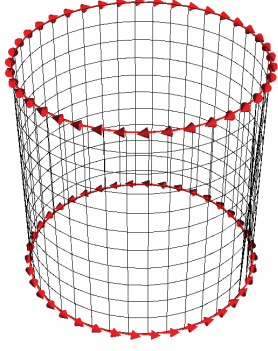


FIG. 1. (color on-line) The edge current associated with the Chern insulator described in the text. There are $40/12$ sites in the circumferential and height directions respectively. The direction of the current is illustrated by the red arrows. The length of arrows is proportional to the magnitude of the current. To make the plot easier to understand we have omitted the weak current away from the edge.

three dimensional Euclidean space (\hat{n}^3 is the local surface normal).

Let us warm up by studying the surface of a cylinder. We build a coordinate system as follows: $x(u, v) = \cos u$, $y(u, v) = \sin u$, $z(u, v) = v$. where $0 \leq u < 2\pi$ and $-1 \leq v \leq 1$. Thus we have a cylinder of height 2 and radius 1. The local frame is defined by

$$\begin{aligned}\hat{n}^1(u, v) &= \partial_v \vec{r}(u, v) \\ \hat{n}^2(u, v) &= \partial_u \vec{r}(u, v) \\ \hat{n}^3(u, v) &= \hat{n}^1(u, v) \times \hat{n}^2(u, v),\end{aligned}\quad (6)$$

where $\vec{r}(u, v) = (x(u, v), y(u, v), z(u, v))$. Set u, v to a set of discrete values corresponding to the square lattice we substitute Eq. (6) into Eq. (5) then into Eq. (4). We diagonalize the resulting Hamiltonian numerically and compute the expectation value of the current operator

$$j_{1,2} = \psi_{i,j}^\dagger \tau_{i,j}^{1,2} \psi_{i,j}. \quad (7)$$

In Fig. (1) we plot the result. As expected counter-propagating chiral edge currents are found on the two opposite edges.

Now we are ready for the Mobius strip. The coordinate system we use is

$$\begin{aligned}x(u, v) &= \left(1 + \frac{v}{2} \cos \frac{u}{2}\right) \cos u \\ y(u, v) &= \left(1 + \frac{v}{2} \cos \frac{u}{2}\right) \sin u \\ z(u, v) &= \frac{v}{2} \sin \frac{u}{2}.\end{aligned}\quad (8)$$

Using Eq. (6), Eq. (5) and Eq. (4) we construct the Hamiltonian and numerically diagonalize it. In Fig. (2) we first present the result when all bonds across a line segment are removed. We note that a pair of co-propagating edge currents are localized on the cut. Their presence is

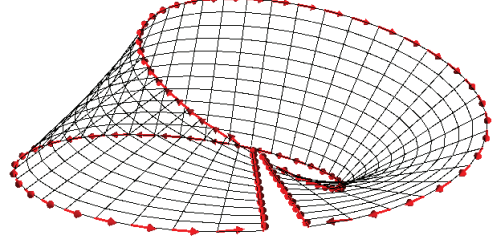


FIG. 2. (color on-line) The edge current associated with the Chern insulator on a Mobius strip. There are 40×12 sites, and all bonds across a line segment are removed. Again, to make the plot easier to understand we have omitted the weak current away from the edge.

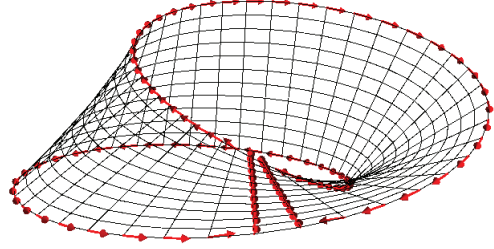


FIG. 3. (color on-line) The edge current associated with the Chern insulator on a Mobius strip. There are 40×12 sites. To make the plot easier to understand we have omitted the weak current away from the edge.

due to the orientation flip across the cut. As a result the chirality of the Chern insulator reverses across the cut. This is similar to the edge current produced at the location of magnetic field reversal in the quantum Hall effect. Because the edge currents at the cut are *co-propagating*, sealing the cut has no effect on them. The current pattern after the cut is sealed is shown in Fig. (3). It is worthy to note that while geometrically there is no singularity on a Mobius strip, in defining the chirality of the Chern insulator it is necessary to choose a cut across which the direction reverses.

Because the above statement is a bit subtle we further explain it as follows. The Chern insulator studied in our paper is fundamentally equivalent to the integer

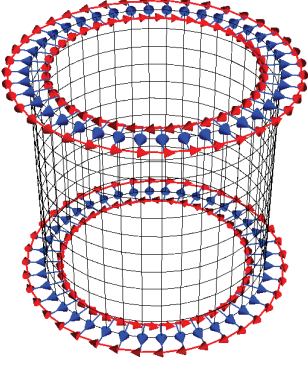


FIG. 4. (color on-line) The edge current associated with the Z_2 insulator on a cylinder. The blue arrows indicate the direction of local S^z axis. The red arrows at the top/bottom of the blue ones illustrate the current associated with $S^z = \pm 1$, respectively. There are 40×12 sites, and to make the plot easier to understand we have omitted the weak current away from the edge.

quantum Hall insulator realized by two dimensional electron gas under strong magnetic field. The chirality in the Chern insulator is analogous to the magnetic field direction in the quantum Hall effect. The question we posed concerning the edge state also applies if we place an integer quantum Hall liquid on a Mobius strip. In the following we explain the fact that while, as a geometric object, the Mobius strip is perfectly smooth, it is impossible to assign local orientation to it smoothly. In connection to the quantum Hall liquid, the local orientation is the local normal direction with respect to which the sign of the Hall conductivity is defined. Indeed, Hall conduction is a local phenomenon; the sign of the Hall conductivity can be defined as $\vec{E} = \sigma_{xy} \hat{n} \times \vec{J}$ where \vec{J} is the current, \hat{n} is the local normal direction, and \vec{E} is the electric field. Clearly reversing \hat{n} changes the sign of σ_{xy} . Mathematically the Mobius strip is a “non-trivial Z_2 fiber bundle with S^1 as the base space”. The associated principal bundle has Z_2 as fiber space. Choosing a local orientation corresponds to picking a “local section” of this principle fiber bundle. The fact that the Mobius strip is topologically non-trivial implies that there exists obstruction to gluing together the local sections smoothly. This is why the Mobius strip is non-orientable, and it is also why a discontinuity (cut) in the direction of local orientation must exist. This cut is not dissimilar to the branch cut in complex analysis. By locally reversing the direction of the orientation we can move the cut around,

however we can never get rid of it. Choosing a particular cut corresponds to picking a specific configuration of local orientations.

Topologically the important thing is not where the cut is, rather it is the necessary existence of a cut. The cut can be anywhere; in this paper we simply pick a particular coordinate system which in turn dictates a particular configuration of local normal direction. In the case of quantum Hall effect, the cut is fixed once the magnetic field configuration is fixed. In other words it is the mag-

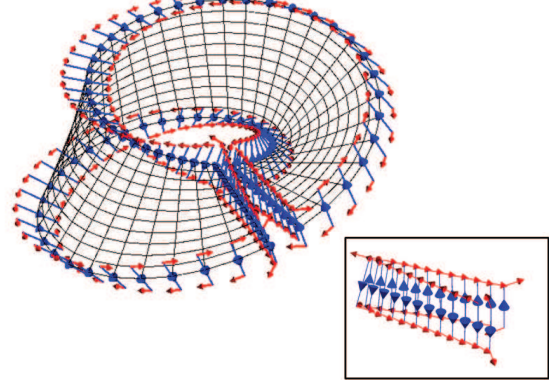


FIG. 5. (color on-line) The edge current associated with the Z_2 insulator on a Mobius strip. Bonds across a line segment are removed. The meaning of blue and red arrows are the same as in Fig. (4). There are 40×12 sites, and to make the plot easier to understand we have omitted the weak current away from the edge. The inset zooms in at the currents near the cut. Note for each spin component there is a pair of counter-propagating current.

netic field that breaks the symmetry between different locations along the Mobius strip. Similar phenomena occurs when one try to construct a coordinate system for a sphere. While a sphere is perfectly smooth, however it is not possible to choose a coordinate system so that it is everywhere non-singular. In this case it is because the total Gauss curvature of the sphere is 4π which cause obstruction to constructing non-singular global coordinate.

Next we study the Z_2 insulator on the Mobius strip. The momentum space Hamiltonian in \mathbb{R}^2 is given by

$$\mathcal{H}(\mathbf{k}) = d_1(\mathbf{k})\tau^1 \otimes I + d_2(\mathbf{k})\tau^2 \otimes I + d_3(\mathbf{k})\tau^3 \otimes \sigma^3, \quad (9)$$

where I is the 2×2 identity matrix. The corresponding real space version is

$$H = -\frac{1}{2} \sum_{i,j} \left[i(\psi_{i+1,j}^\dagger \tau^x \otimes I \psi_{i,j} + \psi_{i,j+1}^\dagger \tau^y \otimes I \psi_{i,j}) + \psi_{i+1,j}^\dagger \otimes \sigma^z \psi_{i,j} + \psi_{i,j+1}^\dagger \tau^z \otimes \sigma^z \psi_{i,j} + h.c. \right] + \sum_{i,j} \psi_{i,j}^\dagger \tau^z \otimes \sigma^z \psi_{i,j}. \quad (10)$$

In defining Eq. (10) on the Mobius strip we define the lo-

cal τ and σ Pauli matrices, $\tau_{i,j}^\mu$ and $\sigma_{i,j}^\mu$ in the same way

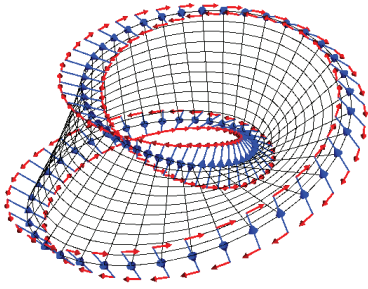


FIG. 6. (color on-line) The edge current associated with the Z_2 insulator on a Möbius strip. The meaning of blue and red arrows are the same as in Fig. (4). There are 40×12 sites, and to make the plot easier to understand we have omitted the weak current away from the edge.

as in Eq. (5). We also start by studying the edge current pattern on the cylinder. As shown in Fig. (4) there are a pair of time-reversal conjugate, counter-propagating edge currents at each edge. Here blue arrows indicate the direction of local S^z axis. The red arrows at the top/bottom of the blue ones illustrate the current associated with $S^z = \pm 1/2$, respectively.

At last we study the Z_2 insulator on the Möbius strip. Again, we begin by removing the bonds across a line segment. The associated current pattern is shown in Fig. (5). The meaning of blue and red arrows are the same as in Fig. (4). The inset zooms in at the currents near the cut.

It is important to note that for each spin component there is a pair of counter-propagating current. As a result, when the cut is sealed they are allowed to back scatter against each other and hence gaps out the associated edge modes. The result with the cut sealed is shown in Fig. (6). As expected the edge currents associated with the cut are completely removed.

Topologically this is because in defining the Z_2 insulator we need a “director” rather than a vector at each point of the Möbius strip. While it is impossible to assign a smooth vector orientation across the Möbius strip, it is possible to assign a seamless “director” to specify the axis of spin quantization. In summary we have studied the edge current distribution of the Chern and Z_2 insulators on the Möbius strip. The current pattern of the Chern insulator clearly detects the twist, while that of the Z_2 insulator does not. This reveals an interesting interaction between the topology of the electronic structure and that of the substrate. The fact that the Z_2 topological insulator can be seamlessly put on a Z_2 fiber bundle (the Möbius strip is a Z_2 fiber bundle over a circle) is particularly interesting. The mathematical meaning of this needs to be clarified in the future.

Acknowledgment: We are in debt to Geoffrey Lee for explaining to us the mathematical meaning of the

chirality cut. We also thank Hong Yao for helpful discussions. LTH acknowledges the supports by (i) NSFC Grant No. 11074143, (ii) the Program of Basic Research Development of China Grant No. 2011CB921901, and (iii) China Scholarship Council and the Doctoral Short-Term Visiting-Abroad Foundation of Tsinghua University, Beijing. DHL is supported by DOE grant number DE-AC02-05CH11231.

-
- ¹ J. Moore, Nature Physcs, **5** 378 (2009); M.Z. Hasan, MZ and C.L. Kane, Rev. Mod. Phys. **82**, 3045 (2010); X.-L. Qi and S.-C.Zhang, Physics Today, **63**, 33 (2010).
- ² D. J. Thouless, M. Kohmoto, M. P. Nightingale, and M. den Nijs **49**, 405 (1982).
- ³ X.-L. Qi, T. L. Hughes, and S.-C. Zhang, Phys. Rev. B **78**, 195424 (2008).
- ⁴ C. L. Kane and E. J. Mele, Phys. Rev. Lett. **95**, 226801 (2005); C. L. Kane and E. J. Mele, Phys. Rev. Lett. **95**, 146802 (2005).
- ⁵ J.E. Moore, L. Balents, Phys. Rev. B 75, 121306(R) (2007).
- ⁶ R. Roy, Phys. Rev. B **79**, 195322 (2009).
- ⁷ L.Fu, C. L. Kane, and E. J. Mele, Phys. Rev. Lett. **98**, 106803 (2007); L. Fu and C. L. Kane, Phys. Rev. B **76**, 045302 (2007).
- ⁸ B. I. Halperin Phys. Rev. B **25**, 2185 (1982)
- ⁹ Yasuhiro Hatsugai Phys. Rev. Lett. **71**, 3697 (1993).
- ¹⁰ B. A. Bernevig, T. L. Hughes, and S.-C. Zhang, Science **314**, 1757 (2006).
- ¹¹ M. Konig, S. Wiedmann, C. Brune, A. Roth, H. Buhmann, L.W. Molenkamp, X.-L. Qi, S.-C. Zhang, Science, **318**, 766, (2007).
- ¹² L. Fu, C.L. Kane, and E.J. Mele, Phys. Rev. Lett. **98**, 106803 (2007).
- ¹³ D. Hsieh et al., Nature 452, 970 (2008); D. Hsieh et al., Science 323, 919 (2009); Y. Xia et al., Nature Physics 5, 398 (2009); Y. L. Chen et al., Science, 1173034 (June 11, 2009).
- ¹⁴ F. D. M. Haldane Phys. Rev. Lett. **61**, 2015 (1988).
- ¹⁵ D.-H. Lee, Phys. Rev. Lett. **103**,196804, (2009).